RI | 9504

REPORT OF INVESTIGATIONS/1994

Electrowinning of Neodymium From a Molten Oxide-Fluoride Electrolyte

By D. K. Dysinger and J. E. Murphy

UNITED STATES DEPARTMENT OF THE INTERIOR

BUREAU OF MINES

U.S. Department of the Interior
Mission Statement

As the Nation's principal conservation agency, the Department of the Interior has responsibility for most of our nationally-owned public lands and natural resources. This includes fostering sound use of our land and water resources; protecting our fish, wildlife, and biological diversity; preserving the environmental and cultural values of our national parks and historical places; and providing for the enjoyment of life through outdoor recreation. The Department assesses our energy and mineral resources and works to ensure that their development is in the best interests of all our people by encouraging stewardship and citizen participation in their care. The Department also has a major responsibility for American Indian reservation communities and for people who live in island territories under U.S. administration.

Report of Investigations 9504

Electrowinning of Neodymium From a Molten Oxide-Fluoride Electrolyte

By D. K. Dysinger and J. E. Murphy

UNITED STATES DEPARTMENT OF THE INTERIOR
Bruce Babbitt, Secretary

BUREAU OF MINES

International Standard Serial Number
ISSN 1066-5552

CONTENTS

ILLUSTRATIONS

TABLES

UNIT OF MEASURE ABBREVIATIONS USED IN THIS REPORT

A	ampere	kW	kilowatt
A/cm^2	ampere per square centimeter	lb/in^2	pound per square inch
A•h	ampere hour	min	minute
°C	degree Celsius	mL	milliliter
°C/min	degree Celsius per minute	μm	micrometer
cm^2	square centimeter	mol pct	mole percent
g	gram	pct	percent
g/min	gram per minute	V	volt
h	hour	wt pct	weight percent
in	inch		

ELECTROWINNING OF NEODYMIUM FROM A MOLTEN OXIDE-FLUORIDE ELECTROLYTE

By D. K. Dysinger[1] and J. E. Murphy[2]

ABSTRACT

In this U.S. Bureau of Mines study, neodymium metal of 99.8 pct purity was prepared by electrolysis of Nd_2O_3 salts dissolved in a molten fluoride electrolyte. The metal was electrowon in a molten state at current efficiencies of 50 to 60 pct. Oxygen and carbon were the major impurities detected in the product. During operation of the small-scale laboratory cell, a number of technical problems including anode effect, low oxide solubility in the electrolyte, high neodymium metal solubility, reactivity of the metal with the cell materials, and back reaction of the metal with the anode gases were encountered. Approaches to improve cell operation and prospects for commercial adoption of the electrolytic production of neodymium metal are discussed.

[1]Chemical engineer.
[2]Supervisory physical scientist.
Reno Research Center, U.S. Bureau of Mines, Reno, NV.

INTRODUCTION

Permanent magnets made from $Nd_{16}Fe_{76}B_8$ show a large improvement in performance over the existing high-energy Sm-Co-based magnets. The raw materials for the Nd-Fe-B magnets are also significantly less expensive and more plentiful than the Sm-Co materials. As a result, demand for neodymium should continue for the foreseeable future.

In the 1960's and early 1970's, Morrice investigated the electrolytic preparation of neodymium metal from the oxide salt (*1*).[3] The electrolysis was conducted in a thermal gradient cell in which the metal was electrowon in a high-temperature zone and dripped from a molybdenum rod cathode. A thermal gradient was maintained between the top and bottom of the cell by cooling the cell bottom to 750° C, which established a "salt skull" between the molten electrolyte and the graphite cell bottom. The temperature of the top portion of the cell was maintained above the melting point of the metal, 1,024° C, by alternating current flowing between two anodes. Metal electrowon in the hot zone dripped from the cathode rod and collected as nodules on the frozen skull avoiding contact with cell bottom, thus preventing reaction between the metal and the graphite cell materials. The metal was subsequently recovered by cooling and crushing the cell contents and handpicking the nodules from the crushed salt. Morrice concluded that the thermal gradient cell was required for successful electrolysis of neodymium.

Subsequent to Morrice's work, other researchers have investigated electrolysis from chloride (*2*) and fluoride-oxide electrolytes to produce neodymium metal (*3-4*). Ohashi of SEC Co. described a cell for commercial electrolysis of Nd_2O_3 in a fluoride electrolyte similar to Shedd's (*3, 5*). Tamamura reported on commercial produc-tion of Nd-Fe alloys by electrolysis of NdF_3 (*4*).

The present work was undertaken to demonstrate the viability of collecting the dripped neodymium metal as a molten product on a hearth in the cell bottom. The molten neodymium metal could be recovered from the cell by tapping or siphoning, as would be done industrially. Similar systems for lanthanum, cerium, and misch metal have been demonstrated by previous U.S. Bureau of Mines researchers (*5-7*).

The electrolytic production of neodymium metal is attractive for several reasons. A higher purity product may be possible than is presently produced by calciothermic reduction, Nd_2O_3 is cheaper and easier to prepare than the fluoride salt, and the process is continuous.

CELL DESIGN

The cells that were used in the early phase of the research were machined from electrolytic-grade graphite. A schematic of the graphite cell is illustrated in figure 1. The upper chamber of the cell was 5.25 in diam and 2.375 in deep. Eight 0.75-in-diam graphite anodes extended into the cell from a refractory SiO_2 cover plate and were immersed 1.25 in. The cathode was a 0.125-in-diam tungsten rod that extended 2.5 in into the melt. Anode-to-cathode spacing was 1.375 in. The lower chamber of the cell contained a molybdenum receptacle in which the molten metal product was collected.

The Nd_2O_3 was fed intermittently in 4-g batches into the graphite cells. The graphite material was not attacked by the fluoride electrolyte during melting, but was severely attacked by the bath during electrolysis, causing several problems. Carbon dust from the crucible collected on the bath surface causing short circuiting. Severe attack and penetration of the salt into the pores of the graphite cell walls required breaking of the crucible to recover the salt.

Stainless steel was also tested as a cell material and proved to be superior in performance to graphite. The stainless steel cell was 4.75 in diam and 5 in deep with a

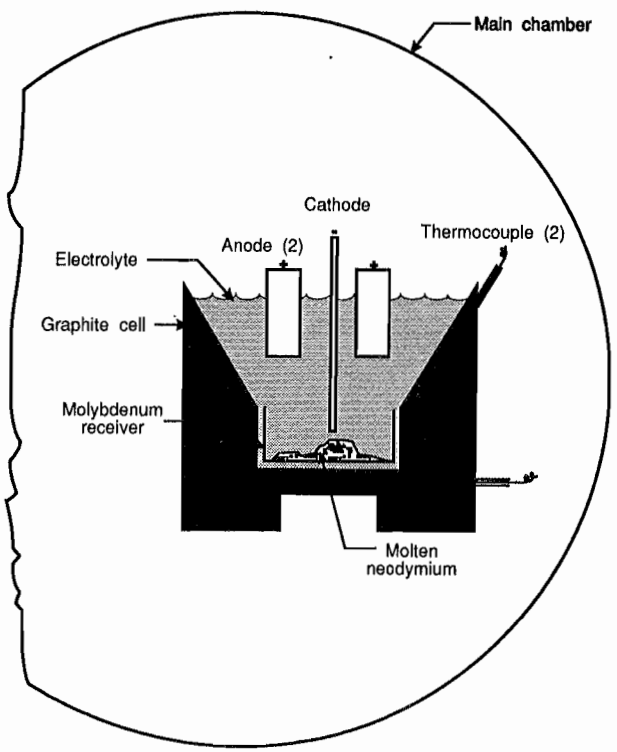

Figure 1.—Electrolytic cell overview schematic view.

[3]Italic numbers in parentheses refer to items in the list of references at the end of this report.

wall thickness of 0.15 in. In the test work with the stainless cell, the oxide was fed continuously.

Since neodymium forms a low melting point alloy with stainless steel, contact between the container and the molten neodymium metal product, which dripped from the cathode and collected on the cell bottom, had to be avoided. Metal collection receptacles, formed from molybdenum sheet, were used to isolate the cell bottom from the product.

Anodes for the stainless cell were fabricated from 1/8-in flat graphite plate and bolted to a stainless hanger bracket for suspension into the bath. The anodes were 1-in-wide strips and were immersed 1 to 2 in into the electrolyte.

Molybdenum was also tested as a cell material but did not provide a measurable advantage over the lower cost stainless steel cell.

FURNACE AND ANCILLARY EQUIPMENT

A resistance furnace was used to heat the cell to the operating temperature. The heating elements were four SiC rods. Power was supplied by a 220-V variac with a maximum power output of 5 kW. The furnace was lined with refractory brick and was housed in a copper sheet casing that was placed inside an inert atmosphere glove chamber to prevent oxidation of the cell materials. The copper casing was water cooled to control the inside temperature of the glove chamber. The furnace power was interlocked with the cooling water to shut the furnace down if water flow was interrupted.

A powder feeder constructed from 304 stainless steel was used to continuously feed the sparingly soluble Nd_2O_3. An open hopper held the oxide, which was transported from the hopper by a 3/8-in-diam wood auger through an 8.5-in-long barrel to the cell. The feeder was continuously vibrated to prevent caking and bridging of the fine oxide powder. The auger speed was controlled by a variable-speed motor and control unit.

EXPERIMENTAL RESULTS

OXIDE SOLUBILITY

A series of experiments was conducted to assess the solubility of Nd_2O_3 in the fluoride electrolyte. The electrolytes were composed of NdF_3, ranging from 5 to 20 mol pct, combined with a mixture of LiF-CaF_2 at 8:2 mole ratio. Sixty-gram samples of the electrolyte, mixed with 6 g Nd_2O_3, were placed in a 1-in-diam graphite crucible. The samples were heated to 1,030° C for 1 h. A 1/4-in-diam graphite tube with a 1/8-in internal tapered bore was used to sample the molten electrolyte. The graphite sample tube was inserted approximately 1/4 in into the molten salt, a slight vacuum was applied, and a sample was drawn into the tube where the salt froze. The sample was then analyzed for oxygen by vacuum fusion. The results are presented in figure 2.

The oxygen analysis indicates that Nd_2O_3 solubility is approximately 3 wt pct in a salt mixture containing 5 mol pct NdF_3, and increases to 3.9 wt pct in a mixture containing 20 mol pct NdF_3. These values are in general agreement with previous work on rare earth oxide solubilities in molten fluoride electrolytes (*8*).

CELL OPERATION DURING BATCH FEEDING

During initial experiments, Nd_2O_3 was batch fed to the cell with a ladle, which held approximately 4 g. The frequency of addition was varied to provide sufficient oxide, assuming 100-pct current efficiency, to operate the cell at anodic current densities up to 2.0 A/cm^2.

The operational data for a representative cell utilizing batch oxide feed are presented in table 1.

The composition of the electrolyte was, in mole percent, NdF_3, 10; LiF, 72; and CaF_2, 18. In a typical experiment, electrolysis was conducted at 1,050° C for 160 A•h. The

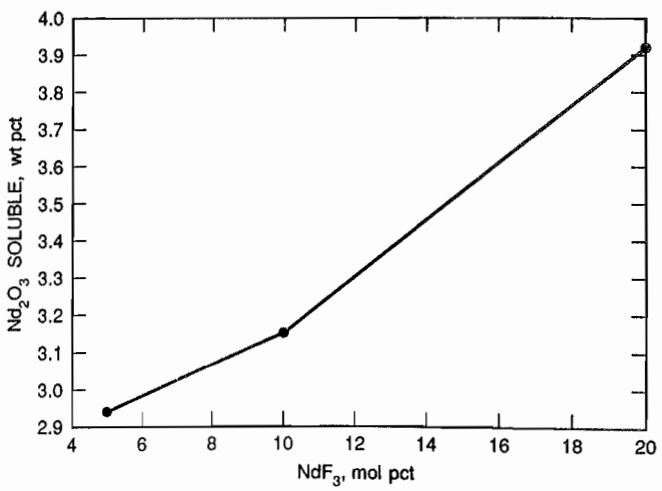

Figure 2.—Measured solubility of Nd_2O_3 in Nd-Li-Ca fluoride electrolyte.

neodymium metal was recovered as a consolidated chunk of metal assaying 99.8 pct Nd metal. Typical analyses of neodymium metal produced are shown in table 2. The impurities are within acceptable limits for magnet use. The major impurities, in weight percent, were carbon, 0.08; oxygen, 0.02; and iron, 0.1.

Table 1.—Operating data for electrolytic cell during batch feeding of Nd_2O_3

Operating temperature	°C	1,030
Anodic surface area	cm^2	91.2
Anodic current density	A/cm^2	0.30
Cathodic surface area	cm^2	2.5
Cathodic current density	A/cm^2	10.97
Electrolysis	A•h	124.0
Nd_2O_3 feed	total g	354.0
Mean feed rate	g/min	1.3
Theoretical current	A	37.35
Mean current	A	27.37
Neodymium metal recovered	g	117.0
Current efficiency	pct	52.7
Oxide utilization	pct	38.6

Table 2.—Analysis of neodymium metal produced during continuous Nd_2O_3 feed experiment

Element	*pct*
Neodymium	99.8
Iron	.1
Carbon	.08
Oxygen	.02

The effect of oxide addition rate on sustainable current density is shown in figure 3. The maximum sustainable current density was determined by adjusting the cell voltage to the highest level without inducing anode effect where the cell current would drop to zero (see discussion under the "Fluoride Electrolysis" section). The lower line on the figure is a fitted line for the experimental data, and the upper line is the theoretical current density expected at 100-pct oxide utilization and 100-pct current efficiency. Figure 3 shows that the sustainable current density, under batch feed conditions, was limited to a maximum of approximately 0.6 A/cm^2. At batch addition rates above roughly 0.75 g/min, the theoretical and actual current density diverge, indicating a buildup of undissolved oxide in the cell bottom. The data indicate that long-term cell operation may be possible by limiting the current density to approximately 0.1 to 0.15 A/cm^2.

Figure 4 is a plot of actual and theoretical cumulative ampere hours as a function of cumulative Nd_2O_3 fed. The theoretical ampere hours are defined as the ampere hours expected at 100-pct current efficiency and 100-pct oxide utilization. Figure 4 provides a perspective on the accumulation of undissolved Nd_2O_3 in the cell. When the cell current efficiency is taken into account, overall oxide utilization was 38.6 pct. The tail on the right end of the experimental line in figure 4 shows that electrolysis was continued after feeding was stopped. The cell operation during this period was erratic, and the sustainable cell current decreased continuously as the available oxide in the cell was consumed.

At cell current density above approximately 0.3 A/cm^2, the cell operation tended to be fairly erratic. Anode effect occurred suddenly and constant adjustment of the cell voltage was required. The heavy oxide, with a specific gravity of 7.4, settled rapidly to the cell bottom in the bath, which has a specific gravity of approximately 2.8. Once on the cell bottom, dissolution was apparently very slow.

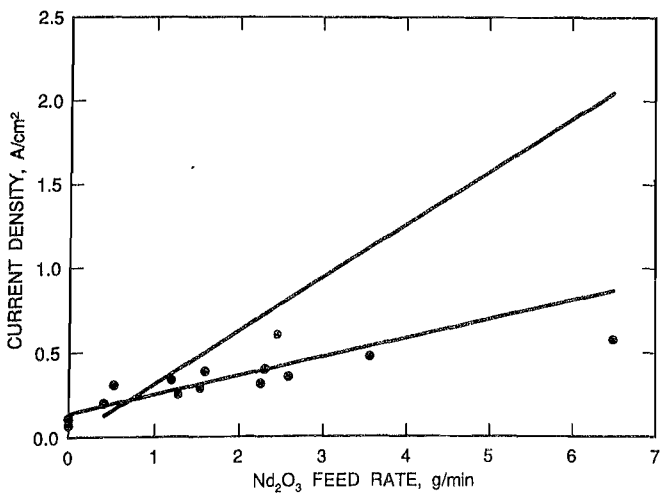

Figure 3.—Actual and theoretical current density versus Nd_2O_3 feed rate during batch feeding.

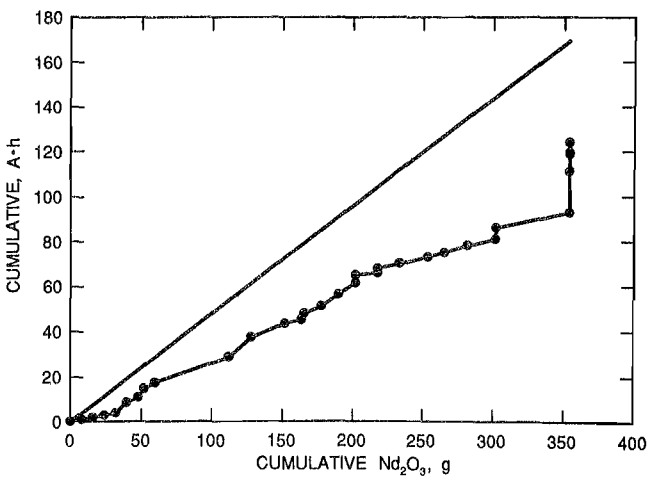

Figure 4.—Actual and theoretical cumulative ampere hours versus cumulative grams of Nd_2O_3 fed during batch feeding.

CELL OPERATION DURING CONTINUOUS FEEDING

To operate at higher current density and current efficiency and to alleviate the buildup of undissolved oxide in the cell bottom, a feeder was designed and constructed to feed continuously at a controlled rate. Continuous feeding increased sustainable anodic current density, increased current efficiency, and dramatically improved the overall operation of the cell.

The theoretical sustainable anodic current density, assuming 100-pct oxide utilization and 100-pct current efficiency, was calculated for continuous feed rates from 0.5 to 1.6 g of Nd_2O_3/min. The actual sustainable current density ranged from 0.27 to 1 A/cm² and is shown as a function of the calculated theoretical current density in figure 5. The solid line represents the theoretical and the points represent the experimental results.

The experimental current densities shown in figure 5 were the maximum sustainable current densities. Attempting to increase current density by increasing the cell voltage resulted in anode polarization and cessation of the electrolysis. As shown, the sustainable current density and calculated current densities were highly correlated.

CURRENT EFFICIENCY

Cell current efficiency was found to be related to the linear spacing between the anodes and cathode. Anode-cathode spacings (ACS) of 0.625, 0.75, 1.25, 1.375, and 2.0 in were tested. The effect of ACS is illustrated on figure 6. The data indicate over a 25-pct improvement in cell current efficiency is obtained by increasing the ACS from 0.625 to 1.25 in. Little improvement in current efficiency is indicated by increasing the ACS from 1.25 to 2.0 in.

FLUORIDE ELECTROLYSIS

Initial test work also included electrolysis of the fluoride salt. Although NdF_3 is more difficult and expensive to prepare, the high solubility of the fluoride electrolyte is attractive because of the problems associated with the low oxide solubility.

The graphite cell described earlier was used for these experiments. The cathode was a 7- by 0.125-in-diam tungsten rod and the cell operating temperature was maintained at 1,030° C, 6° C above the melting point of neodymium. Initial tests were performed using a 20 mol pct NdF_3-80 mol pct LiF eutectic bath having a melting point of approximately 720° C, but no coalesced metal was recovered. A series of tests was conducted in which the bath was spiked with neodymium metal in an attempt to induce coalescence of the electrowon metal. A net loss of metal to the bath was experienced indicating a significant solubility of the metal in the bath.

High-purity neodymium was electrowon from an electrolyte mixture containing 5 mol pct NdF_3 and 95 mol pct LiF. The electrowon metal dripped from the cathode and coalesced into a pool in the cell bottom. The anodic current density was 0.1 A/cm² and current efficiency was 33 pct. The metal button assayed 0.08 wt pct C.

In these experiments, the anode reaction was rate limiting. At anodic current densities above approximately 0.1 A/cm², complete polarization of the anode occurred. Anode effect is a well-known phenomenon in electrolytic systems utilizing fluoride-based electrolytes (*9*). The assumed anodic reaction in the fluoride system involves the

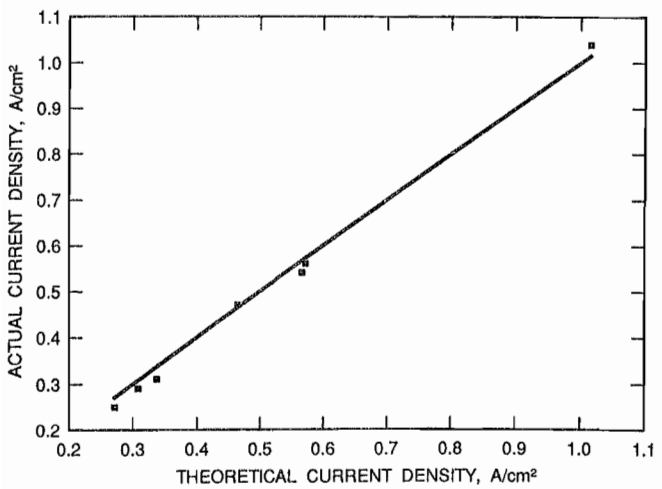

Figure 5.—Actual and theoretical current density during continuous feeding.

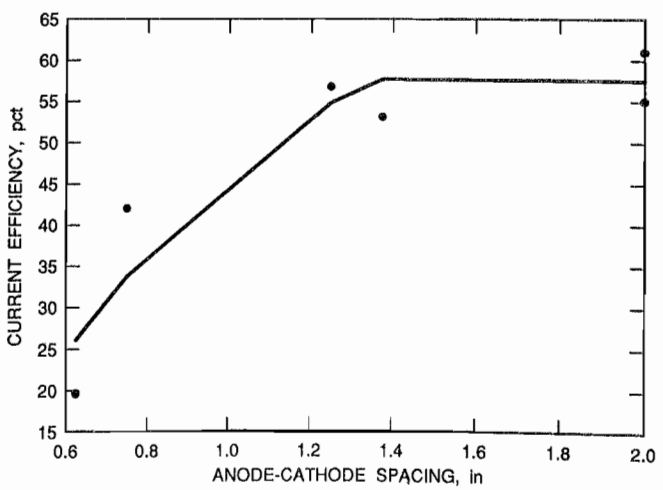

Figure 6.—Current efficiency versus anode-cathode spacing.

oxidation of carbon and the formation of tetrafluoromethane, CF_4. A simplified reaction is

$$4NdF_3 + 3C \rightarrow 4Nd + 3CF_{4(g)}\uparrow. \qquad (A)$$

Anode effect is attributed to the formation of an envelope of CF_4 gas that formed on the anode surface. The anode ceased to be wetted by the electrolyte causing the current to drop near zero under constant voltage conditions. Limited current was reestablished by increasing the voltage but resulted in electrical arcs at the anode surface. Electrolysis under these conditions resulted in anode spalling into the bath and very low current efficiency. Once anode effect occurred, the applied voltage had to be reduced below deposition potential to reestablish electrolysis.

COMPOSITE ANODES

Composite anodes, an intimate mixture of carbon and Nd_2O_3, were investigated as an alternative approach for electrowinning neodymium metal. It was anticipated that the composite anode would overcome the problem of low Nd_2O_3 solubility. Ashland Chemical A-240,[4] a low softening point petroleum pitch binder, was selected as a binder for making the electrodes.

The composite anodes were prepared as follows: A weighed quantity of A-240 binder was liquified in a 250-mL alumina crucible at 200° C. The liquid binder and Nd_2O_3 were blended into a homogenous mixture by stirring using a stainless steel impeller. Sufficient Nd_2O_3 was added to ensure the desired residual carbon content was present in the finished anode. The binder and oxide mixture was allowed to cool and then placed in a hydraulic press. The mixture was pressed at 2,500 to 3,500 lb/in^2 pressure and 150° C for 4 h. The resultant green anode was a 1-in-diam by 1.5-in-long cylinder. The green anode was then fired, unsupported, in an argon atmosphere. The green anode was heated from ambient to 1,050° C at a rate of 2° to 3° C/min. The temperature was held at 1,050° C for 4 h, after which the furnace was shut off and allowed to cool at a natural rate. The binder lost approximately 51 wt pct through volatilization. The resultant composite anode was structurally rigid and electrically conductive. In most anodes, visible, fine hairline cracks indicated the heating rate was too fast.

The composite anode was clamped with a stainless steel holder and electrolyzed in a bath of 10 mol pct NdF_3, 81 mol pct LiF, and 9 mol pct CaF_2. The bath temperature was maintained at 1,030° C and the cathode, a 1/8-in-diam tungsten rod, was inserted into the bath from overhead. A molybdenum receiver was located in the bottom of the graphite crucible for collection of electrowon metal.

In tests using anodes of approximately 6 wt pct C, anode effect was not present at anodic current densities of 1.25 A/cm^2. The anodes, however, disintegrated after only 5 to 8 A•h of electrolysis.

Anodes containing approximately 10 to 24 pct C by weight were significantly more durable and held up well under electrolysis conditions. However, anode effect was experienced at relatively low current density. For example, sustainable current density decreased from 0.28 A/cm^2 using anodes containing 12 wt pct C to approximately 0.15 A/cm^2 at 24 wt pct C.

DISCUSSION

CURRENT EFFICIENCY

Several possible mechanisms may have contributed to the low current efficiencies recorded in the experiments. The mechanisms include back reaction, dissolution and "fogging" of neodymium metal into the electrolyte either as a metallic solution or a metal "fog" (*10*), reduction of other bath components, and the small scale of the experimental cell.

As shown by the data in figure 6, current efficiency was influenced by the separation between the anode and cathode, suggesting back reaction between electrowon metal and carbon oxide anode gases may have been occurring. The neodymium metal was electrowon near the bath surface and dripped from the cathode rod onto the cell bottom. The proximity of the electrowinning zone to the rising gas bubbles increased the likelihood of gas-metal contact. Two possible reactions are as follows:

$$2Nd + 3CO_2 + NdF_3 \rightarrow 3NdOF + 3CO \qquad (B)$$

and

$$3CO_2 + 2Nd \rightarrow Nd_2O_3 + 3CO. \qquad (C)$$

Back reaction between electrowon metal and anode gases has been experimentally demonstrated to be the primary mechanism of current inefficiency in the aluminum cell (*11*). X-ray diffraction analyses of the frozen salt from several experiments indicated that NdOF was the only oxygen-carrying compound in the frozen salt, suggesting back reaction would occur by reaction B.

In situ generation of NdOF through back reaction in the cell between CO_2 and neodymium metal would be expected to increase the maximum sustainable cell current by

[4]Reference to specific products does not imply endorsement by the U.S. Bureau of Mines.

an amount equivalent to the rate of back reaction. However, a near-perfect correlation, illustrated in figure 5, was obtained between the theoretical current density, based on the oxide feed rate, and the actual sustainable cell current density. Attempts to "drive" the cell current above the sustainable levels shown on figure 5 resulted in anode effect. Cessation or simply slowing of the feed rate without decreasing the voltage also resulted in anode effect, usually within 1 to 2 min. Thus, the oxide generated in situ did not allow the cell to operate at higher current, as did an increase in fresh oxide feed rate. Back reaction has not been conclusively demonstrated at the present time and may not be the controlling mechanism.

A second potential factor contributing to the relatively low current efficiency may be dissolution of neodymium metal into the electrolyte. Dissolved metal in the electrolyte impacts current efficiency by decreasing the recoverable metal yield and potentially causes electronic conduction through the electrolyte. The evidence for metal dissolution is anecdotal and derived from the apparent loss of metal "spiked" to the electrolyte prior to electrolysis of a 20 mol pct NdF_3-80 mol pct LiF electrolyte, the appearance of the frozen salt after electrolysis, and the corrosion of the graphite cell wall during electrolysis.

The mechanism by which the metal would dissolve in the fluoride electrolyte is not understood. One possibility is the formation of a "subfluoride" species similar to that observed for the other neodymium halides, which readily form subhalides in the chloride, bromide, and iodide salts (*10, 12*). The greater stability of NdF_3 and the lack of identification of a subfluoride species make its existence appear doubtful.

A similar explanation would be that the neodymium is present as a "fog" in the salt. The postexperiment frozen salt was separated into a top layer of clean electrolyte and a bottom layer of high-density salt consisting primarily of NdOF and electrolyte, identified by X-ray diffraction. Scanning electron microscopy showed neodymium metal distributed throughout the bottom layer in approximately 10-μm blebs.

Whether metal is dissolved or present in the salt as a "fog," the effect on current efficiency would be similar. The tendency for both problems may have been exacerbated by not cathodically protecting the electrowon metal product in the cell bottom.

Although a buildup of metal in the electrolyte can be expected to cause electronic conduction, this was only overtly identifiable when the cell was operated at 1,080° C or higher. Electronic conduction as the controlling current carrying mechanism appeared to cease when the cell temperature was reduced to 1,050° C.

A third potential contributing factor to reduced current efficiency is coreduction of lithium and calcium, in spite of unfavorable thermodynamics. Some evidence of lithium production was noted by the collection of Li_2O on the furnace components above the electrolyte.

Another potentially contributing, and possibly most important, factor is the small scale of the experimental cell, which may have magnified and aggravated the extent of all of the above mechanisms. Low current efficiency of laboratory cells is common and widely reported in the literature for aluminum molten salt electrolysis experiments (*13*).

The cause of the current inefficiency has not been determined with any certainty during the course of this investigation, and the mechanisms elucidated above are only potential causes.

OXIDE UTILIZATION

Another problem that warrants discussion is low oxide utilization in the cell. From the cell data shown in figures 3 and 5, there were large differences in sustainable current densities between batch and continuous oxide feeding. Current density was limited to 0.5 A/cm^2 with batch feeding of the oxide. Sustainable current density increased to 1.0 A/cm^2 during continuous feeding, which should be quite acceptable for an industrial cell operation. During continuous feeding, the oxide is introduced at a much lower instantaneous rate than during the slugging that occurs during batch feeding. The steady, even introduction of the oxide resulted in better contact between the oxide and electrolyte and improved cell performance.

Even with continuous feeding, however, a portion of the oxide did not dissolve and settled to the cell bottom where it did not appear to dissolve at any appreciable rate. An industrial cell could not operate on a long-term basis with a buildup of undissolved oxide. Point feeding of the oxide is believed to have aggravated the problem in the experimental cell. Spreading the oxide evenly over the surface of the bath would maximize the contact with the electrolyte and maximize solubilization.

An attempt was made to heat the oxide before adding it to the cell to improve the dissolution rate. However, the heated oxide became "gummy" and would not feed properly. As a result, preheating the oxide feed was not pursued. Intuitively, preheating the oxide would aid in the rate of dissolution since the solubility is directly dependent on temperature. A commercial cell could be designed with an oxide dissolution chamber in which the oxide would be preheated and mixed with electrolyte before adding to the cell.

The small scale of the experimental apparatus is believed to have aggravated the problem of oxide solubility. Since the oxide settles at a fixed terminal velocity, a deeper cell would allow proportionately more time for heating and dissolution than the shallow dimensions of the experimental cell.

In a large cell, neodymium would most likely be electrowon into a molten cathode pool at the cell bottom. It is possible the oxide would be reduced at the cathode. Such cathode reduction of undissolved species is known to occur (*14*). Electrowinning into a molten cathode of neodymium would also serve to keep the metal product cathodic and would separate the metal from the anode gas.

CONCLUSIONS

Electrowinning neodymium from Nd_2O_3 has potential as a low-cost production process. Large-scale, continuous cell operation appears feasible despite the very high operating temperature and low oxide solubility. The metal produced during the relatively short-duration tests was 99.8 pct, which is probably feasible on a larger scale. Other conclusions drawn from the study are as follows:

1. The thermal gradient cell previously described by Morrice is not critical to neodymium electrowinning. Results similar to Morrice's (*1*) were obtained in this study with a smaller scale cell. The metal was electrowon in a molten state demonstrating the process can be continuous instead of the batch operation thought necessary by the earlier researchers.

2. The low oxide solubility and slow oxide dissolution rate are major problems of the process. Larger scale cells can be expected to be more efficient based on aluminum industry experience and work on other rare earth oxides. Considerations for improving the solubility and dissolution rates are

   a. Preheating of the oxide feed to increase the dispersion and dissolution characteristics of the oxide in the bath.

   b. Optimization of the electrolyte to improve the overall solubility.

   c. Development of a feeder system to introduce the oxide evenly over the bath surface.

3. A cathodically protected pool of molten neodymium metal in the cell bottom is probably required to reduce the effect of metal redissolution and solubility in the electrolyte. The molten metal cathode would be expected to reduce back reaction with the anode gases but must be isolated from graphite or other carbon components because of the formation of neodymium carbide.

4. The results of this study show a relatively high current density of 1 A/cm^2 can be attained with no indication of reduced cell efficiency when compared to lower current density. As a basis for comparison, the current density of high-production aluminum cells is maintained near 1 A/cm^2.

5. Considering the fast settling velocity and slow dissolution rate of the oxide, deep insertion of the anodes into the bath may improve the oxide utilization.

6. The electrolyte composition should be investigated for maximum oxide solubility and minimum neodymium solubility.

7. The feasibility of electrowinning neodymium in a molten state at high current density has been demonstrated by the results of this study. However, a scaled-up cell must be operated for a reasonable time on a continuous basis to determine if the problems noted in this study will be manageable on a commercial-scale operation.

REFERENCES

1. Morrice, E., and T. A. Henrie. Electrowinning High-Purity Neodymium, Praseodymium, and Didymium Metals From Their Oxides. BuMines RI 6957, 1966, 11 pp.

2. Chambers, M. F., and J. E. Murphy. Electrolytic Production of Neodymium Metal From a Molten Chloride Electrolyte. BuMines RI 9391, 1991, 7 pp.

3. Ohashi, K. Technologies and Economic Aspects of Using Dy or NdFeB Magnets. Paper presented at the Impact of NdFeB Materials on Permanent Magnet Users, Producers, and Raw Material Suppliers (June 4-5, 1990). Gorham Advanced Materials Inst., Seattle, WA, 16 pp.

4. Tamamura, H., T. Shima-Oka, and M. Utsunomiya. New Industrial Process for Electrowinning of Nd-Fe Alloy. Paper in Proceedings of 177th Meeting of the Electrochemical Society (Montreal, Canada, May 6-11, 1990). Electrochem. Soc., 1990, 16 pp.

5. Shedd, E. S., J. D. Marchant, and T. A. Henrie. Electrowinning and Tapping of Lanthanum Metal. BuMines RI 6882, 1966, 10 pp.

6. ____. Continuous Electrowinning of Cerium Metal From Cerium Oxides. BuMines RI 6362, 1964, 12 pp.

7. Shedd, E. S., J. D. Marchant, and M. M. Wong. Electrowinning Misch Metal From a Treated Bastnasite Concentrate. BuMines RI 7398, 1970, 11 pp.

8. Porter, B., and E. A. Brown. Determination of Oxide Solubility in Molten Fluorides. BuMines RI 5878, 1961, 8 pp.

9. Mantell, C. L. Electrochemical Engineering, 4th ed. McGraw-Hill, 1960, pp. 359-369.

10. Bredig, M. A. Mixtures of Metals With Molten Salts. Molten Salt Chemistry, ed. by M. Blander. Wiley, 1964, pp. 367-425.

11. Hamlin, J. D., and N. E. Richards. Studies of the Anode Gas From the Hall-Heroult Cell. Paper in Proceedings of 1st International Symposium on the Extractive Metallurgy of Aluminum. Wiley, 1963, pp. 51-63.

12. Bloom, H. The Chemistry of Molten Salts. W. A. Benjamin, Inc., 1967, pp. 149-150.

13. Sterten, A., S. Rolseth, E. Skybakmoen, A. Solheim, and J. Thonstad. Some Aspects of Low-Melting Baths in Aluminum Electrolysis. Ch. in Light Metals 1988. TMS, 1987, pp. 663-670.

14. Haver, F. P., D. L. Bixby, and M. M. Wong. Aqueous Electrolysis of Lead Chloride. BuMines RI 8276, 1978, 11 pp.

INT.BU.OF MINES,PGH.,PA 29934

☆ U.S. Government Printing Office: 1994—509-008 — 00031